From:
The Institute of Anatomy,
University of Bergen,
Norway

A QUANTITATIVE ANALYSIS OF THE NUMERICAL DENSITY AND THE DISTRIBUTIONAL PATTERN OF PRISMS AND AMELOBLASTS IN DENTAL ENAMEL AND TOOTH GERMS

VII. THE NUMBERS OF CROSS-SECTIONED AMELOBLASTS AND PRISMS PER UNIT AREA IN TOOTH GERMS

by

GISLE FOSSE

INTRODUCTION

It has never been possible to prove or disprove that each prism is the product of one and the same ameloblast. Therefore it has not been possible to give a clear definition of the numerical relation between ameloblasts and prism rods in a given location of a tooth germ during amelogenesis.

Previous authors have come to different conclusions concerning this relationship.

Mummery (1924) found that the processes of Tomes were divided into bundles that intertwined to produce the greater part of the enamel matrix, while each single prism was the product of several ameloblasts.

Gottlieb (1943) maintained that the peculiar course of groups of rods in some places rendered it improbable that each prism was formed by only one ameloblast. He expressed the opinion that in such places the rods were crystallization products in the originally homogeneous matrix. Gottlieb did not offer any opinion concerning the numerical relation between ameloblasts and prisms during amelogenesis.

Orban et al. (1943) concluded from their investigations that each prism is the product of one ameloblast. The long axes of the ameloblasts and prisms are at an angle to each other.

Tomes' processes are hexagonal in cross-section.

Chase (1948) wrote as an answer to Gottlieb's conclusions that the numerical relation between ameloblasts and prisms is a constant; each ameloblast corresponds to one prism. Moreover, prisms are present in all stages of enamel development, from the earliest matrix stage to completely mineralized enamel.

Besides, Chase stated that each rod runs unbroken from the amelodentinal junction towards the outer surface and that one rod was produced throughout by one ameloblast, provided that each prism is produced by an individual ameloblast.

In an earlier paper *Chase* (1927) mentioned that he had tried to calculate the number of ameloblasts of a given tooth germ, intending to compare the result with the number of prisms on the outer surface of an identical kind of tooth. The method applied did not yield useful results, however.

Watson and *Avery* (1954) found by electronmicroscopic studies that one ameloblast is responsible for one prism rod and the interprismatic substance on one side of the prism.

Quigley (1959) examined hamster enamel by the electron microscope. He arrived at the conclusion that the fibrils of the interprismatic substance constitute a continuous network and that the prisms are formed secondarily in this.

Quigley stated that each one of the »cytoplasmic projections» which are present in a higher number per unit area than the ameloblasts, produces a prism rod. He also suggested that the tortuous course that is followed by some prism groups, might be explained in this way without assuming that lateral currents have occured. Furthermore, the growing surface of the enamel layer is compensated for by a gradual increase of such projections, and not of ameloblasts.

In this way, according to Quigley, a growing number of supplementary prisms must arise towards the outer enamel surface. In support of this latter standpoint he stated that with the very high magnifications applied by him, even the smallest increase of prism diameter would be perceptible. He had never seen such an increase, however.

Ten Cate (1961) did not deal with the numerical relation between ameloblasts and prisms. His object was to establish whether new ameloblasts were recruited from the stratum intermedium. He used the conception »insinuating cells» which signified cells that originated in stratum intermedium and were transformed to ameloblasts. As an average he found 4 such insinuating cells per 30 ameloblasts, and concluded that new ameloblasts originate from stratum intermedium.

Rönnholm (1961) studied different stages of the amelogenesis electronmicroscopically. He stated that in the earliest stages of amelogenesis, the distal ends of the ameloblasts are folded with long thin projections pointing towards the dentine (*Mummery*, 1924; *Quigley*, 1959). At a more advanced stage the distal ends get smooth and the so called Tomes' processes are formed, one for each ameloblasts. But several ameloblasts are responsible for the forming of each prism rod. It was not explicitly stated whether the author meant that the total number of ameloblasts consequently is higher than the total number of prisms within a given region.

Rönnholm (1961) stated that the angle between the axes of the ameloblasts and prisms is generally between 45° and 90°. He also stated that cross-sectioned ameloblasts are hexagonal.

Helmcke (1964) reconstructed the form and course of individual prism rods in simian enamel. The reconstructions demonstrated that while some rods ended, others arose in the course towards the outer surface. He concluded that it was difficult to conceive that one ameloblast gives rise to one prism and determines its spatial course.

Boyde (1964) wrote that the number of ameloblasts equals the number of prisms, but morphologically one prism needs not be a direct »prolongation» of one ameloblast. Up to four ameloblasts may have contributed to the production of one prism. The same ameloblasts are also partaking in the genesis of the adjacent prisms.

If it were accepted that several ameloblasts are responsible for the forming of one prism rod (*Rönnholm*, 1961; *Boyde*, 1964), it would hardly be a logical necessity that the numbers of ameloblasts and prisms rods should be equal in a given region of a tooth germ. Besides, since *Mummery* (1924) and *Quigley* (1959) explicitly claimed that the numbers were different, the present author felt that it might be useful to reexamine the numerical relation between ameloblasts and prisms using a new approach.

By sectioning tooth germs in series of sections which were planoparallel to the layers of ameloblasts and enamel matrix it should be possible to compare the numerical densities of the cross-sectioned ameloblasts and prism rods by means of the method described in part III.

MATERIAL

5—6 month-old human foetuses were placed in Bouin's fluid immediately post partem. A few hours later the maxilla was extirpated in toto and allowed to remain in the fixative for a period of 3—4 days.

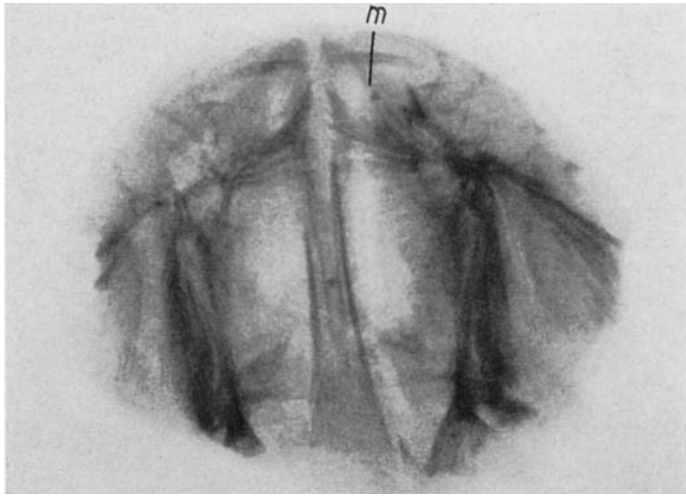

Fig. 1. Roentgenograph of the maxilla of a 6-month-old human foetus. The incisal edges of the first incisors are seen as two straight darker bands near the upper margin of the picture. A median plane designated by the letter »m» has been drawn on one of the germs.

After completion of fixation the specimens were roentgenographed, Fig. 1, and decalcified in a 5.2 % solution of HNO_3 for 48 hours. The maxilla was then carefully divided along the median palatinal suture. Each half was dehydrated and embedded in paraffin.

Kittens were killed by chloroform and the jaws were extirpated and placed in Bouin's fluid. They were subjected to the same procedure as the human jaws.

Two mature human deciduous maxillary central incisors were included in the material. They were to serve as control material for the human tooth germs.

METHODS

Serial sectioning and microphotography of the germs of the maxillary human deciduous central incisor

Using the X-ray picture as a guide, the specimen was orientated so that the sectioning plane would be in the sagittal labio-lingual planes of the tooth germ of the deciduous central incisor. Also the depth of the series was determined by the X-ray picture, since the series was to end in the median plane of the germ.

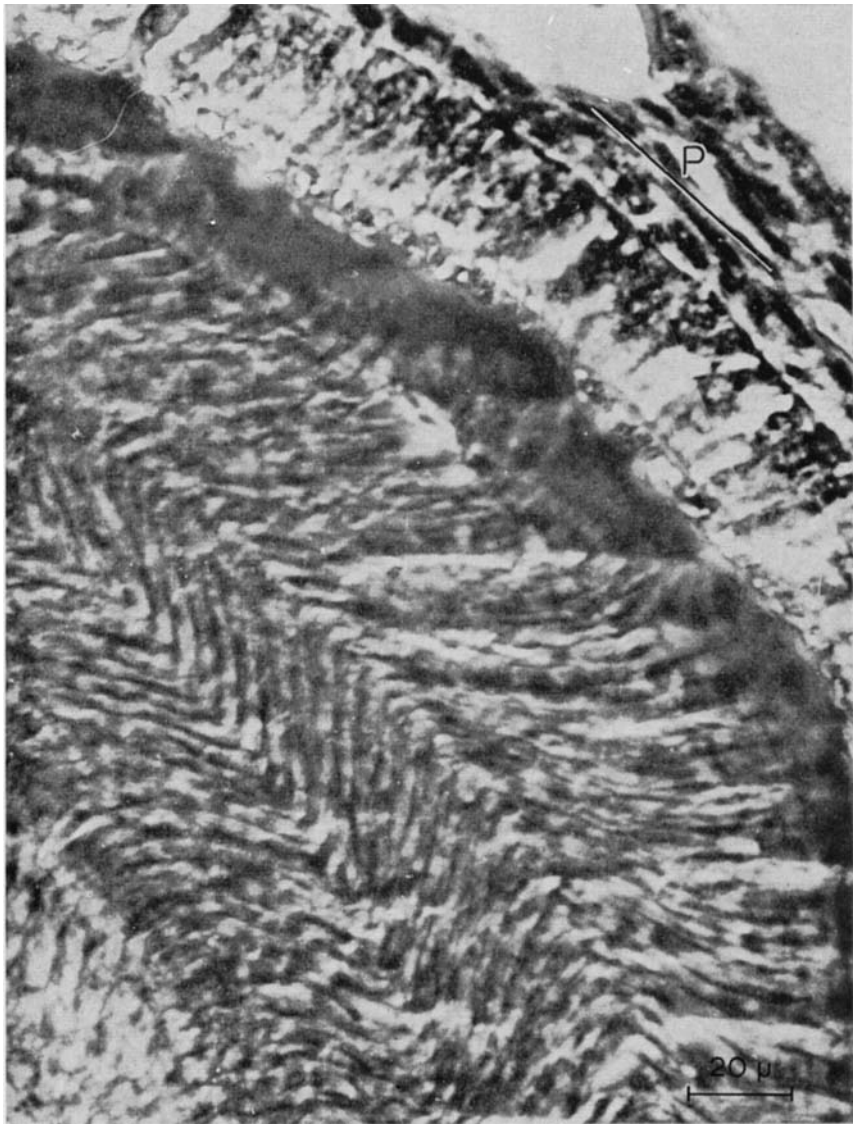

Fig. 2. A median section through the ameloblastic layer and the enamel matrix of the tooth germ of a human maxillary first deciduous incisor. The photomicrograph covers an area near the labial surface and the incisal edge. In this region a new series was prepared consisting of tangent sections perpendicular to the median plane and planoparallel to the amelodentinal junction. The direction of the tangent sections is designated by P.

From the last section of such a series was determined the angle between the longitudinal axis of the germ and the sectioning plane of a new series. The new series was to consist of sections orientated 90° to the median plane and approximately planoparallel to the inner enamel epithelium. Such a series will later be called a tangent series, and the separate sections, tangential sections.

Fig. 2 represents a photomicrograph of the last section in the median plane. The letter P designates the chosen direction of a tangential section 90° to this plane.

On the section plane of the paraffin block which contained the remaining half of the tooth germ, was ruled a straight line in the tangential direction previously determined in the median section and illustrated in Fig. 2. This line was ruled under a binocular dissecting microscope, centrifugally to the inner enamel epithelium. The different tissue elements of the germ were plainly visible on the unstained paraffin surface.

The block was then fastened to the microtome chuck so that the tangential line was parallel to the knife edge, the original section plane being vertical to the feeding direction.

The tangential sections of the human tooth germs were thus bordered at one side by a straight margin representing the last median section plane. A rectangular region bordered at one side by this margin was photographed in each section in an attempt to follow a straight line towards the amelodentinal junction. The photographed regions covered the central part of the sectioned ameloblastic layer and the matrix layer throughout the series. The sections were photographed by the Zeiss phase contrast microscope using the 16× objective. The section thickness was 6 μ.

Fig. 4 is a representation of a section from one of the human embryonal tangent series. The lower straight border of the tissue represents the original median section.

Serial sectioning and microphotography of feline tooth germs

The paraffin block containing one half of the maxilla was orientated so that the section plane would be perpendicular to the occlusion plane and parallel to a line between the central incisor and the canine.

Thus the series of tangential planes was cut directly and a predetermination of the location of the intersection point between section plane and ameloblastic layer was impossible. The longitudinal axis of the tooth germ was determined by the cut surface through the median palatinal suture which was visible as a straight border to the section.

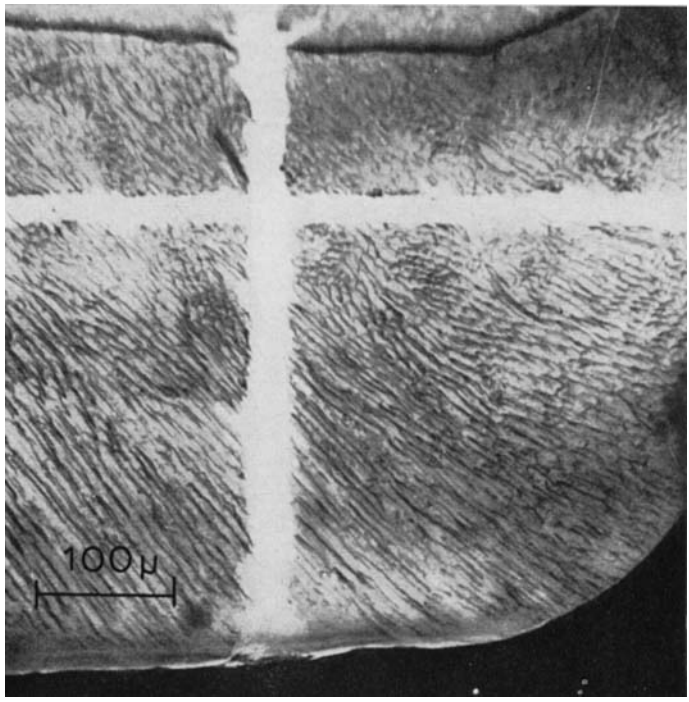

Fig. 3. A median section through the enamel of a mature human maxillary first deciduous incisor. The photomicrograph covers an area near the labial surface and the incisal edge. The white line perpendicular to the amelodentinal junction was the guide line of the series of etched enamel surfaces which were to be perpendicular to the median plane and plano-parallel to the amelodentinal junction.

In an attempt to follow a straight line towards the amelodentinal junction, the regions photographed covered the central part of the circular area of ameloblasts or enamel matrix throughout the series.

The sections were photographed by the Leitz 25× objective. The thickness of the sections was 6 μ.

Serial etching and microphotography of the enamel of human deciduous incisors

In part V this author described how a series of ground enamel surfaces plano-parallel to the amelodentinal junction was prepared in a median tooth section.

The same procedure was followed by the orientation of the series in the enamel of the two incisors. Instead of serial grinding, however, the method of serial enamel etching described in part II was applied.

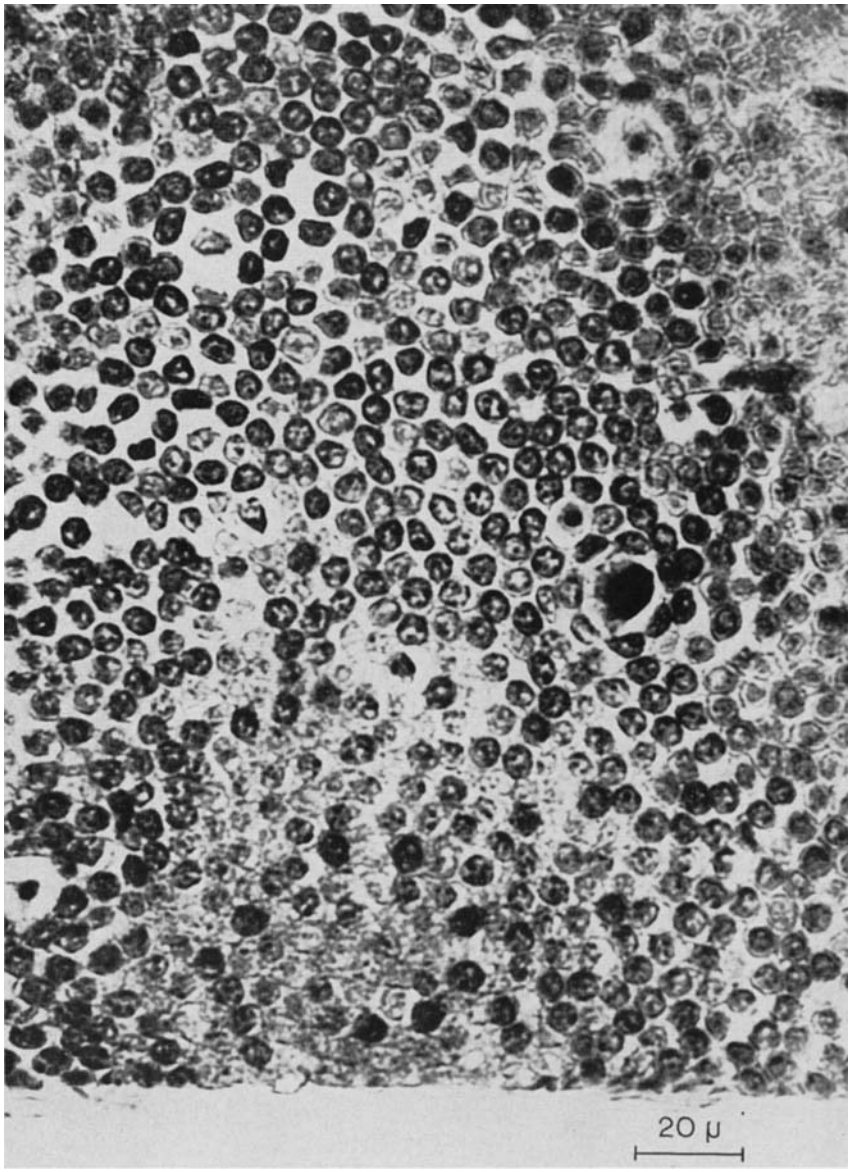

Fig. 4. A tangential section through the ameloblastic layer of the tooth germ whose median section was represented by Fig. 2. The median section plane is seen along the lower border of the photomicrograph.

The interproximate distance between the etched planes of the series in one specimen was 5 μ, and in the other 7 μ.

The series were located in the same position as the tangent series in the human tooth germ. Fig. 3 represents a median incisal segment on the labial surface of one of the two specimens. The line directed perpendicularly to the amelodentinal junction was the guide line, (cf. part V) which served as a reference line while photographing the etched planes.

The etched surfaces were photographed by the Leitz 22× Ultropak objective.

Determination of ameloblastic and prismatic density and pattern

In part III the author described his method of calculating prism density, pattern and diameters by measuring the central distances between pairs of adjacent prisms.

In practice the determination and plotting of the centers of ameloblasts is not different from the plotting of prism centers.

RESULTS

Human tooth germs

Figs. 4, 5 and 6 represent consecutive tangent sections of the tooth germ whose median section was represented by Fig. 2. The series from this tooth germ is called H_1.

Fig. 4 represents the third ameloblastic section. Figs. 5 and 6 represent the first and the sixth of the following 15 matrix sections. The photographs demonstrate the existence of prisms even in the youngest matrix of this germ. The prisms were continuously discernible throughout the matrix.

Fig. 7 represents a photomicrograph of the ameloblasts in this series in a section plane at the level of the nuclei. Fig. 8 represents a photomicrograph of the prisms near the amelodentinal junction of the same series. Both sections were photographed by the 100× immersion objective and the photographs were reproduced with the same magnification. The similarity in size and form is evident.

In Table I are listed the a_{reg}-, $\langle a_{gr}\rangle$-, S_{agr}-, $\langle K\rangle$-, S_K-, $\langle D\rangle$- and S_D-values from H_1. The columns in the table are divided by a horizontal line that separates the upper ameloblastic and the lower prismatic values.

Fig. 9 is a diagrammatic representation of the $\langle a_{gr}\rangle$-values. To each $\langle a_{gr}\rangle$-value in the diagram is added and subtracted the double standard

Table I

Series H_1. The density, the vertical compression of pattern and the central distances of ameloblasts and prisms in the tooth germ of a human deciduous central incisor.

Tissue	Depth in μ	Triangles	Groups	Prisms/mm²			Vert. compr.		Centr. dist.	
				areg	⟨agr⟩	Sagr	⟨K⟩	SK	⟨D⟩	SD
Ameloblasts	0	76	5	28020	28487	1061	1,09	0,34	6,39	0,51
	6	148	10	29305	29138	1708	0,97	0,17	6,25	0,50
	12	106	12	32255	32197	4239	1,03	0,29	5,95	0,54
	18	142	11	34881	34776	3314	0,95	0,19	5,73	0,45
	24	119	17	35826	36423	4001	1,03	0,23	5,65	0,46
	30	59	11	32389	34172	5487	1,04	0,25	5,93	0,60
Prisms	36	88	6	29719	30245	1295	1,07	0,29	6,21	0,45
	42	122	12	26985	27046	2356	0,91	0,15	6,52	0,44
	48	125	13	25833	26724	2854	0,96	0,20	6,66	0,53
	54	104	15	28855	28903	2874	0,99	0,20	6,30	0,48
	60	60	10	28087	29178	5505	0,93	0,17	6,36	0,76
	66	82	12	28703	28763	2832	0,94	0,16	6,32	0,49

deviation. The vertical line separates the ameloblastic and the prismatic values.

Tables II, III and IV and Figs. 10, 11 and 12 represent three different tooth germs of the human deciduous central incisor presenting the values in the same manner as was done for H_1. The three series from these three new specimens will be designated by the symbols H_2, H_3 and H_4.

In all series the average of the compression ratios ⟨K⟩ seemed to approximate the value 1.00, see Tables I, II, III and IV.

Feline tooth germs

Figs. 13 and 14 represent the ameloblasts and the prisms in a series from a feline deciduous incisor. The similarity in size is evident.

The two photomicrographs were reproduced in the same scale and were taken by the 100× objective.

Table V presents the data from the series of a feline tooth germ. Fig. 15 is a graphical representation of the ⟨agr⟩-values with the double standard deviations added and subtracted. This series will be designated by F.

The average of the ⟨K⟩-values of the series seemed to approximate a value slightly below 1.00.

Table II

Series H_2. The density, the vertical compression of pattern and the central distances of ameloblasts and prisms in the tooth germ of a human deciduous central incisor.

Tissue	Depth in μ	Triangles	Groups	Prisms/mm²			Vert. compr.		Centr. dist.	
				a_{reg}	$\langle a_{gr} \rangle$	S_{agr}	$\langle K \rangle$	S_K	$\langle D \rangle$	S_D
Ameloblasts	0	68	17	35491	35331	3268	0,92	0,23	5,68	0,47
	6	51	14	35726	35843	3350	1,06	0,30	5,66	0,44
	12	65	7	30956	31599	2701	1,09	0,28	6,08	0,53
	18	54	5	33846	34004	4345	1,02	0,26	5,81	0,54
	24	107	12	28196	28923	4055	0,94	0,26	6,37	0,57
Prisms	30	60	9	25160	25394	2115	0,90	0,22	6,74	0,59
	36	77	8	30119	31944	4122	0,96	0,16	6,17	0,49
	42	59	9	34070	37007	5507	0,95	0,24	5,78	0,61
	48	40	6	33659	33523	2971	1,07	0,25	5,84	0,41

Table III

Series H_3. The density, the vertical compression of pattern and the central distances of ameloblasts and prisms in the tooth germ of a human deciduous central incisor.

Tissue	Depth in μ	Triangles	Groups	Prisms/mm²			Vert. compr.		Centr. dist.	
				a_{reg}	$\langle a_{gr} \rangle$	S_{agr}	$\langle K \rangle$	S_K	$\langle D \rangle$	S_D
Amel-oblasts	0	107	13	40910	41317	3543	1,05	0,29	5,29	0,41
	6	130	13	41963	42116	2606	1,00	0,18	5,23	0,34
	12	28	3	36722	40124	7480	1,07	0,32	5,56	0,72
Prisms	18	10	2	39292	40326	3630	1,09	0,12	5,41	0,31
	24	28	7	36953	36367	3730	1,02	0,20	5,57	0,38
	30	48	7	35459	35431	3138	0,99	0,17	5,68	0,44
	36	87	9	35943	36531	3774	1,03	0,17	5,65	0,41
	42	101	11	41366	41385	2975	1,02	0,16	5,26	0,41
	48	84	9	41967	43154	3076	1,10	0,18	5,23	0,30
	54	62	6	37318	38197	3517	1,05	0,17	5,54	0,42

Table IV

Series H_4. The density, the vertical compression of pattern and the central distances of ameloblasts and prisms in the tooth germ of a human deciduous central incisor.

Tissue	Depth in μ	Triangles	Groups	Prisms/mm²			Vert. compr.		Centr. dist.	
				a_{reg}	$\langle a_{gr} \rangle$	S_{agr}	$\langle K \rangle$	S_K	$\langle D \rangle$	S_D
Amel oblasts	0	23	7	28296	28284	3685	1,18	0,38	6,36	0,55
	6	69	10	27076	25995	2569	1,09	0,30	6,50	0,55
	12	8	3	26466	27273	3074	1,14	0,49	6,58	0,54
Prisms	18	25	5	35173	37543	4280	1,01	0,23	5,71	0,44
	24	30	3	34949	35662	2926	1,19	0,27	5,71	0,57
	30	114	10	36404	37151	3976	1,01	0,23	5,61	0,47
	36	49	8	34399	32963	4463	0,96	0,26	5,77	0,44

Table V

Series F. The density, the vertical compression of pattern and the central distances of ameloblasts and prisms in the tooth germ of a feline deciduous incisor.

Tissue	Depth in μ	Triangles	Groups	Prisms/mm²			Vert. compr.		Centr. dist.	
				a_{reg}	$\langle a_{gr} \rangle$	S_{agr}	$\langle K \rangle$	S_K	$\langle D \rangle$	S_D
Amel-oblasts	0	40	4	37946	36801	2265	1,00	0,17	5,50	0,42
	6	88	9	35724	35982	2568	0,91	0,17	5,66	0,42
	12	107	10	36898	37118	3557	0,88	0,13	5,57	0,40
	18	91	8	37857	37888	2650	1,04	0,23	5,50	0,39
Prisms	24	88	10	38317	39373	4380	0,95	0,22	5,47	0,37
	30	126	12	33865	35328	5267	0,95	0,19	5,82	0,42
	36	52	10	37266	37927	3924	0,95	0,13	5,55	0,41
	42	23	5	37260	38538	4414	0,87	0,14	5,55	0,28
	48	11	3	32868	34279	4595	0,92	0,19	5,90	0,52
	54	32	7	43318	42432	3675	0,90	0,17	5,15	0,34
	60	31	6	43662	43543	4978	0,81	0,08	5,13	0,35
	66	60	9	40794	42649	3707	0,95	0,17	5,30	0,45
	72	73	11	41548	44884	6940	1,02	0,43	5,24	0,56

Human first deciduous incisors

Figs. 16—19 represent photomicrographs of the last four etched and stained enamel surfaces of a human deciduous incisor. This series is called i_1. The interproximate distance between the surfaces was 5 μ. Even with this small distance individual prisms cannot be recognized from one surface to the next (cf. part II).

In the last three surfaces, represented by figs. 17, 18 and 19, tiny circular, densely stained areas appear in the enamel. They are situated not only between, but also within prisms. They are perhaps enamel spindles. The same phenomenon was demonstrated immediately before the breakthrough to the dentine in a series of etched surfaces from a second tooth of the same kind. This latter series is called i_2.

Tables VI and VII and Figs. 20 and 21 represent the two series of etched enamel surfaces. The interproximate distance between the surfaces of i_2 was 7 μ.

The average of the ⟨K⟩-values of the two series seemed to approximate the value 1.00.

Table VI

Series i_1. The density, the vertical compression of pattern and the central distances of prisms in a series of etched enamel surfaces of a human deciduous central incisor. The first line in the table represents the outer enamel surface.

Depth in μ	Triangles	Groups	Prisms/mm²			Vert. compr.		Centr. dist.	
			a_{reg}	⟨a_{gr}⟩	S_{agr}	⟨K⟩	S_K	⟨D⟩	S_K
0	25	7	29907	29621	3036	1,01	0,22	6,19	0,50
255	87	14	27918	28956	3699	1,13	0,31	6,40	0,58
260	64	11	27557	27514	3000	1,10	0,25	6,45	0,46
265	65	12	29308	29520	2983	1,07	0,23	6,25	0,53
270	68	11	28387	29001	4016	1,05	0,18	6,35	0,50
275	64	12	28418	28902	3799	1,07	0,20	6,34	0,57
280	70	11	25714	25709	3732	1,03	0,19	6,67	0,58
285	73	11	26889	26209	4347	1,08	0,22	6,52	0,63
290	46	9	25874	25863	2150	0,89	0,14	6,66	0,47
295	44	10	26348	27138	2792	0,93	0,19	6,60	0,44
300	27	6	27437	26980	2971	0,95	0,14	6,46	0,47

Table VII

Series i_2. The density, the vertical compression of pattern and the central distances of prisms in a series of etched enamel surfaces of a maxillary human deciduous central incisor. The first line in the table represents the outer enamel surface.

Depth in μ	Triangles	Groups	Prisms/mm²			Vert. compr.		Centr. dist.	
			areg	⟨agr⟩	Sagr	⟨K⟩	SK	⟨D⟩	SD
0	36	12	19105	19734	2757	1,13	0,28	7,74	0,70
411	53	12	21407	21748	2850	0,96	0,18	7,32	0,59
418	45	11	21979	23013	2611	0,99	0,15	7,23	0,50
425	74	12	21525	21815	2235	1,06	0,23	7,30	0,54
432	100	16	23198	23358	2461	1,01	0,16	7,03	0,51
439	95	15	24015	24267	2015	1,04	0,14	6,91	0,45
446	86	15	23961	24092	2019	1,02	0,18	6,92	0,53
453	94	14	23841	24267	2848	1,09	0,24	6,93	0,55
460	40	4	24545	26134	3878	1,11	0,21	6,83	0,51

Statistical testing of the ⟨agr⟩-values in the series of the feline and the 4 human tooth germs

In each embryonal series the last ameloblastic ⟨agr⟩-value was t-tested against the first prismatic ⟨agr⟩-value.

If the confidence limit is set arbitrarily at 5 % there was no statistically significant difference between the last ameloblastic and the first prismatic densities in 3 of the series.

An analysis of variance where the pooled ameloblastic values were tested against the pooled prismatic values in each series, was carried out. The difference was not statistically significant for series H_2, whereas the difference was significant for the remaining 4 series on the 5 % level. For H_1 and H_3 this difference manifested itself as higher ameloblastic than prismatic values, whereas for H_4 and F the ameloblastic values were lower than the prismatic values.

In this material the greatest difference between an ameloblastic and a prismatic ⟨agr⟩-value was found in series H_4 where the second section had a density of 25,995 ameloblasts per mm², while the first prismatic section had a density of 37,543 prisms per mm². The ratio between the latter and the first value equals 1.44. This means that for 100 ameloblasts, each corresponding to one prism, one would find 80 ameloblasts each corresponding to two prisms.

By a similar calculation for the extreme values of H_1 one would find that for 100 prisms, each corresponding to one ameloblast, there would be 56 prisms, each corresponding to two ameloblasts. In the present material these ratios represented the maximal differences between the numbers of ameloblasts and prisms in separate sections. These two extremes were inverse.

DISCUSSION

Compared with the graphical representations of the prism densities in the etched surfaces of the two human deciduous incisors the graphical representation of the ameloblastic and prismatic densities in the 5 embryonal series demonstrated considerable variations. There were also variations within each ameloblastic layer. The graphs do not directly indicate that the number of ameloblasts equals the number of prisms in a given area.

To obtain thin and complete sections and to reduce the risk of losing whole sections within one series, the author applied paraffin embedding of the jaws. The paraffin embedding causes shrinking of tissues, however, and probably this shrinking is not equal for the ameloblasts and the enamel matrix. Therefore an artificial difference in $\langle a_{gr} \rangle$-values within each tissue as well as between the tissues might be expected in advance.

The overall difference between the ameloblastic and the prismatic density in each series does not seem to be systematic however, since two of the series demonstrated a positive difference, two others a negative difference, while one of them demonstrated no statistically significant difference at all.

Moreover the testing of the last ameloblastic section against the first prismatic section in each of the 5 series demonstrated no statistically significant difference in density for three of them.

Accordingly, the present author tends to believe that the apparant differences were artificially caused by unsystematic volume changes of tissues during fixation and subsequent treatment of the specimens before the mounting of the sections.

It might be claimed that fixation and mounting technic had caused a volume change in only one of the tissues, thus masking an original real difference in density. This possibility seems improbable, but cannot be repudiated.

In contrast to the embryonal series, volume changes of the structures in the etched and stained enamel surfaces of i_1 and i_2 are inconceivable. In consequence the distribution of the $\langle a_{gr} \rangle$-values in the latter series is quite even.

CONCLUSION

The results of the present investigation did not indicate that the number of ameloblasts per mm² is *systematically different* from the number of prisms per mm² in the same area of a tooth germ.

ACKNOWLEDGEMENTS

This study was carried out at the Institute of Anatomy, University of Bergen. I wish to express my warmest gratitude to W. Harkmark, M.D., professor and head of the Institute, for his unfailing confidence in me and for his kind interest in my work. I also want to thank him for his help concerning the drafting of the manuscript.

I am greatly indebted to S. Tjotta, Ph.D., at the Institute for Applied Mathematics in Bergen, who was always willing to discuss the mathematical methods described in part III, and whose advices were a great help to me.

I am also much obliged to T. Bjerkedal, M.D., for his invaluable help and advices concerning the statistical treatment of the depth measurements described in part II.

Miss E. Ramm, M.Sc., carried out the programming of the electronic computer for the mathematical and statistical treatment of the measured central distances. For this and for her kind and patient help through the different stages of this study, I want to express my deepest gratitude.

I am much obliged to my friend R. Altenau, M.D., at the maternity ward of Haukeland sykehus, who procured the human foetuses used in the study described in part VII.

My assistant Mrs. K. Thue helped me in carrying out the vast number of measurements to be used, and she also punched the data cards. For her patience and conscientious endurance I am greatly indebted.

Mrs. B. Mastrup prepared the paraffin sections of the tooth germs. Mr. Jensen copied the photomicrographs and assisted me in other respects concerning photographic technique. Miss L. Skarstein has drawn all the diagrams.

The manuscript was written in English. The linguistic corrections were carried out by Mrs. C. Flöysand and the typewriting by Miss K. Olsen.

I ask all the persons mentioned to accept my sincere thanks.

SUMMARY

A series of sections planoparallel to the ameloblastic layer was prepared from each of four human tooth germs of the first maxillary deciduous incisor. A fifth series from a kitten's maxillary first deciduous incisor was included. The section thickness was set to 6 μ.

The four human embryonal series were directed towards the amelodentinal junction in the median plane of the germ and on the labial surface near the tip of the incisal edge.

Within each section of a series passing through the ameloblastic and the matrix layer, the number of ameloblasts or prisms per mm² was calculated.

The results concerning these 4 germs presented in graphical form were comparable to the graphs of two series of etched enamel surfaces from two mature human first maxillary deciduous incisors.

The difference between the numerical densities of the ameloblasts and the prisms was treated statistically for each of the 5 germs. The differencee was not statistically significant for one of them, while there was a significantly higher ameloblastic than prismatic density for two germs and a significantly lower ameloblastic than prismatic density for the remaining two. The author assumed that this unsystematic difference was caused by artificial volume changes during the processing of the specimens from fixation to staining.

It was concluded that the findings did not indicate a systematic differenc between the numerical densities of ameloblasts and prisms in a given area of a tooth germ.

RÉSUMÉ

AMÉLOBLASTES ET PRISMES EN COUPE TRANSVERSALE. LEUR NOMBRE PER UNITÉ DE SURFACE DANS DES GERMES DENTAIRES

Quatre germes dentaires humains d'incisives centrales supérieures temporaires ont servi à préparer des séries de coupes parallèles au plan de la couche améloblastique. Une cinquième série a été préparée en utilisant une incisive centrale supérieure temporaire provenant d'un jeune chat. L'épaisseur des coupes était fixée à 6 μ.

Les quatre séries embryonnaires humaines étaient orientées vers la jonction émail-dentine au niveau du plan médian du germe et sur la face vestibulaire près du sommet du bord incisif.

Dans chaque coupe d'une série traversant la couche améloblastique et celle de la matrice, on a calculé le nombre d'améloblastes ou de prismes par mm^2.

La représentation graphique des résultats concernant ces 4 germes était comparable aux représentations graphiques concernant deux séries de surfaces d'émail attaquées par un acide, provenant de deux incisives centrales supérieures humaines à maturité.

La différence entre la densité numérique des améloblastes et celle des prismes a fait l'objet d'un traitement statistique pour chacun des 5 germes. Pour un des germes, la différence n'était pas significative du point de vue statistique, alors que, pour deux des germes, la densité améloblastique était significativement plus élevée que la densité prismatique, et que, pour les

deux derniers germes, la densité améloblastique était significativement plus basse que la densité prismatique. L'auteur suppose que ces différences non systématiques étaient dues à des changements artificiels de volume pendant la préparation des échantillons de la fixation à la coloration.

En conclusion, les résultats n'ont pas indiqué l'existence d'une différence systématique entre le densité numérique des améloblastes et celle des prismes dans une région donnee du germe dentaire.

ZUSAMMENFASSUNG

DIE ANZAHL DER QUERGESCHNITTENEN AMELOBLASTEN UND PRISMEN PER FLÄCHENEINHEIT IN ZAHNANLAGEN

Eine Serie von Schnitten, die planparallel zu der Ameloblastenschicht waren, wurden von jeder von vier mennschlichen Zahnanlagen vom ersten Schneidezahn des Milchgebisses im Oberkiefer geschnitten. Eine fünfte Serie von der Anlage des ersten Schneidezahnes im Oberkiefer eines Kätzchens wurde auch geschnitten. Die Dicke der Serienschnitte war immer 6 μ.

Die vier mennschlichen Serien waren nach der Schmelz-Dentingrenze im Medianplan gerichtet, und nahe an der Schneidekante auf der labialen Seite gelegen.

Innerhalb jedes Schnittes einer Serie die durch die Ameloblastenschicht des jungen Schmelzes ging, wurden die Anzahl der Ameloblasten oder Prismen per mm^2 berechnet.

Die Ergebnisse der vier Anlagen wurden graphisch dargestellt und konnten dann mit den graphischen Darstellungen von den Prismendichtheiten in zwei Serien von angeätzten Schmelzflächen von zwei mennschlichen Schneidezähnen des Milchgebisses im Oberkiefer verglichen werden.

Der Unterschied zwischen den numerischen Dichtheiten der Ameloblasten und der Prismen wurde für jede der fünf Anlagen statistisch geschätzt.

In der Serie einer der Anlagen war der Unterschied nicht statistisch signifikant. In zwei anderen war die Dichtheit der Ameloblasten signifikant grösser als die der Prismen, weil in den zwei letzten Serien die Dichtheit der Prismen signifikant grösser als die der Ameloblasten war.

Der Verfasser war von der Meinung dass dieser unsystematische Unterschied von Veränderungen während des Fixierungs-, Einbettungs- und Färbungsverfahrens verursacht sei.

Es wurde geschlossen, dass die Ergebnisse nicht einen systematischen Unterschied zwischen den Dichtheiten der Ameloblasten und der Prismen in einer bestimmten Region einer Anlage zeigten.

REFERENCES

Boyde A., 1964: The Structure and Development of Mammalian Enamel. Thesis. Depart. of Anat., The London Hosp. Med. Coll., London. In Stencil.

Chase S. W., 1927: The Number of Enamel Prisms in Human Teeth, J. Amer. Dent. Ass., *14:* 491—492.

—»— *S. W.*, 1948: The Development, Histology and Physiology of Enamel and Dentin—their Significance to the Caries Process, J. Dent. Res., *27:* 87—92.

Gottlieb B., 1943: Development and Physiologic Purpose of the Organic Matter of Enamel, J. Dent. Res., *22:* 185—190.

Helmcke J. G., 1964: Kombination von elektronenmikroskopischen und neuen lichtmikroskopischen Untersuchungsmethoden für Strukturen des Zahnschmelzes. Advances fluorine res., *2:* 127—139.

Mummery J. H., 1924: The Microscopic and General Anatomy of the Teeth, 2. ed., Oxford Univ. Press, London.

Orban B., H. Sicher, & J. P. Weinman, 1943: Amelogenesis. A Critique and a New Conception. J. Amer. Coll. Dent., *10:* 13—22.

Quigley M. B., 1959: Electron Microscopy of Developing Enamel Matrix in the Syrian Hamster, J. Dent. Res., *38:* 180—187.

Rönnholm E., 1961: An Electron Microscopic Study of the Amelogenesis in Human Teeth, J. Ultrastruct. Res., *6:* 229—248.

Ten Cate A. R., 1961: Recruitment in the Internal Enamel Epithel as a Factor in the Growth of the Human Tooth Germ, Brit. Dent. J., *110:* 267—273.

Watson M. L., & J. K. Avery, 1954: The Development of the Hamster Lower Incisor as Observed by Electron Microscope, Amer. J. Anat., *95:* 109—161.

Address:
The Institute of Anatomy,
University of Bergen,
Norway

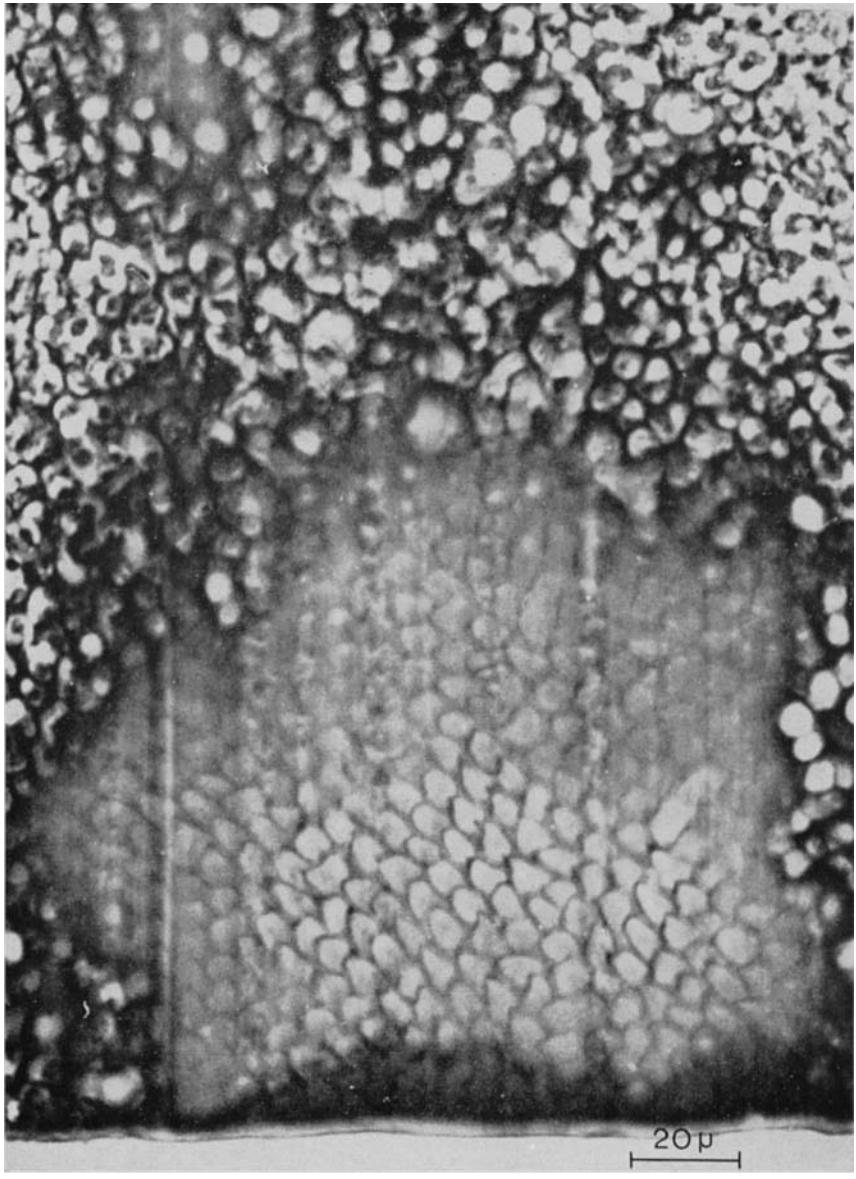

Figs. 5 and 6. The first and the sixth tangent sections through the enamel matrix of the tooth germ whose median section was represented by Fig. 2. The median section plane is seen along the lower border of the photomicrographs. These figures and Fig. 4 represent series H_1.

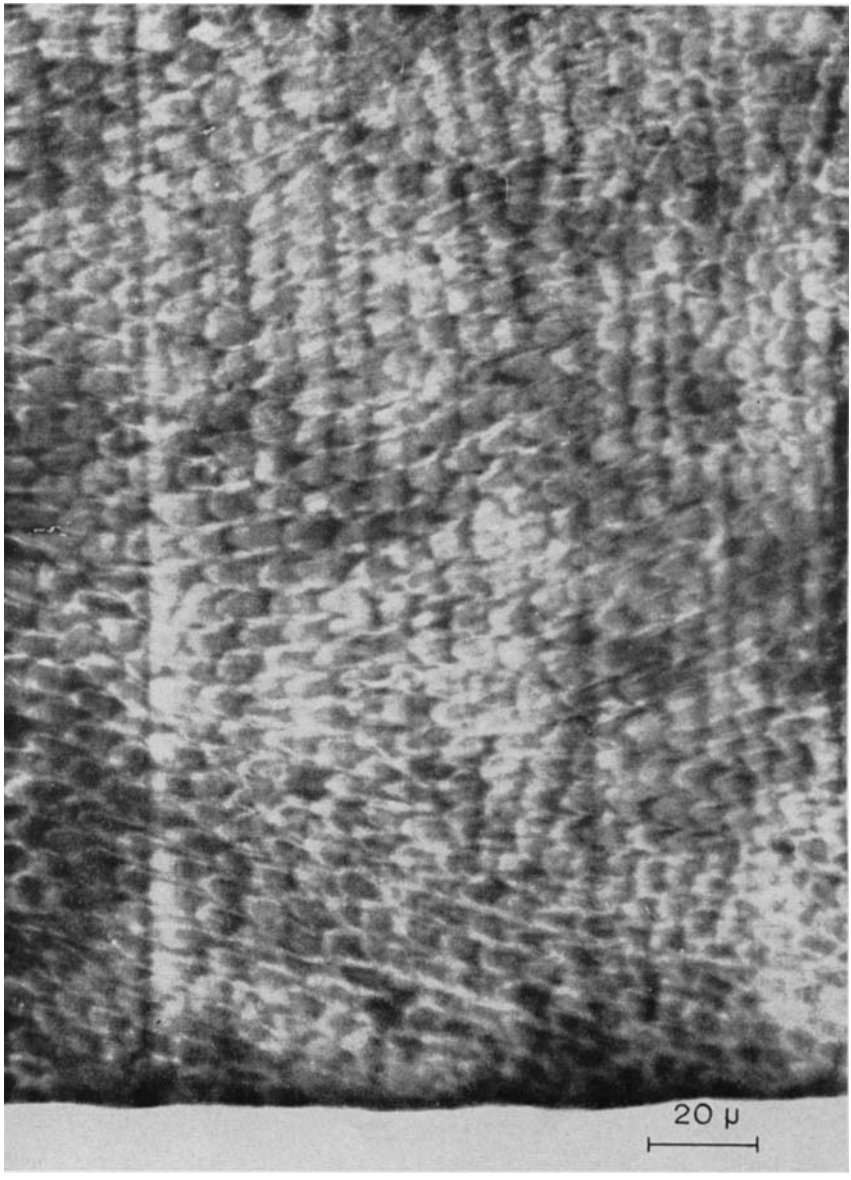

Fig. 6

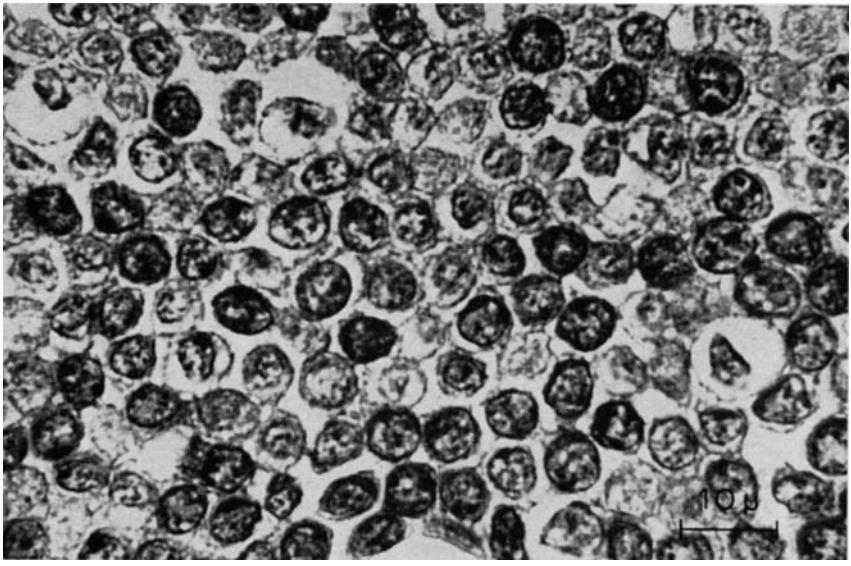

Fig. 7. Tangent section of the ameloblasts in H_1 at the level of the nuclei, photographed by 100× oil imm. obj.

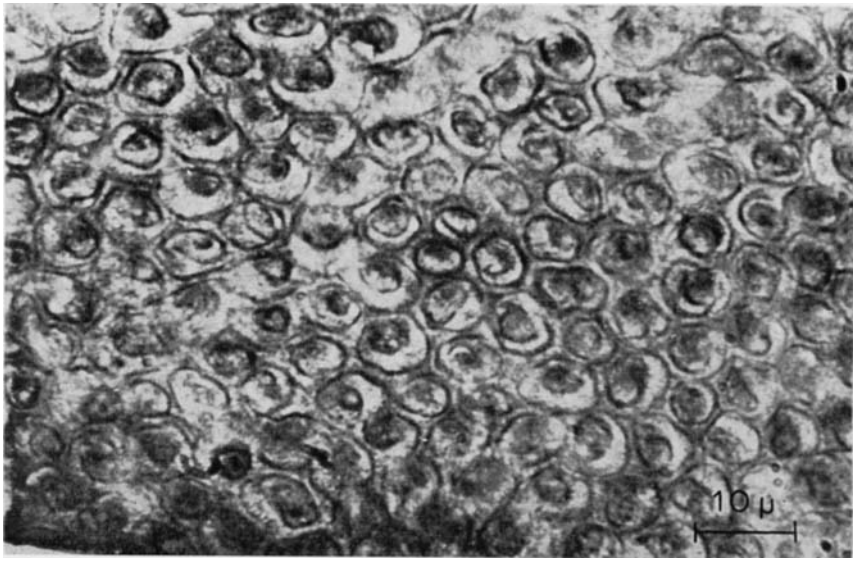

Fig. 8. Tangent section of the prisms in H_1 near the amelodentinal junction photographed by 100× oil imm. obj.

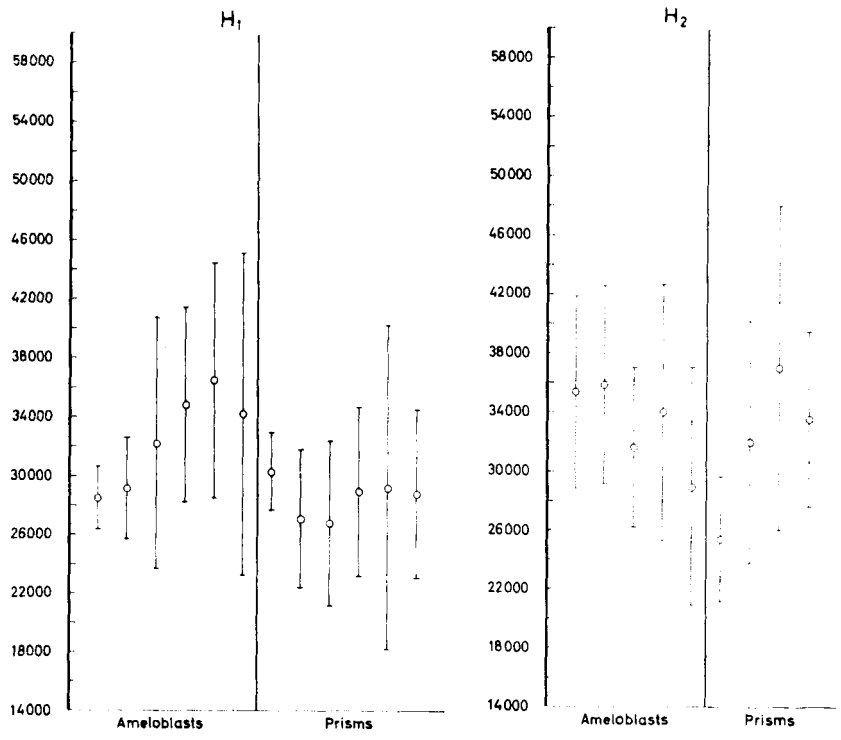

Fig. 9. Graphical representation of the ameloblastic and prismatic densities in a series of sections from a human tooth germ of a maxillary first deciduous incisor. The series is designated by H_1. Each section is represented by the encircled $\langle a_{gr} \rangle$-value and the double standard deviation added and subtracted. Ameloblastic and prismatic values are separated by a vertical line.

Fig. 10. Graphical representation of the ameloblastic and prismatic densities in a series of sections from a human tooth germ of a maxillary first deciduous incisor. The series is designated by H_2. Each section is represented by the encircled $\langle a_{gr} \rangle$-value and the double standard deviation added and subtracted. Ameloblastic and prismatic values are separated by a vertical line.

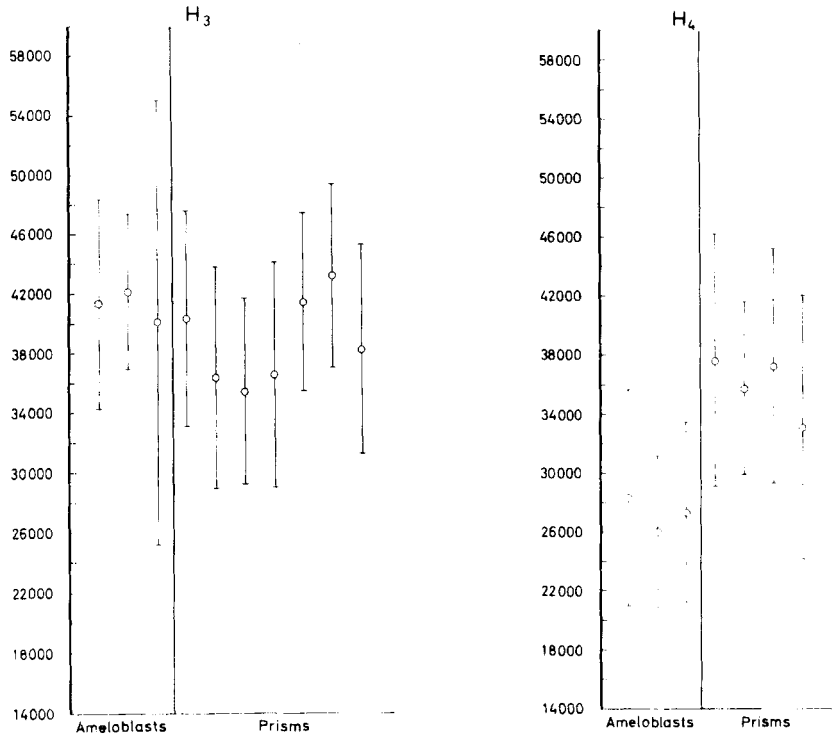

Fig. 11. Graphical representation of the ameloblastic and prismatic densities in a series of sections from a human tooth germ of maxillary first deciduous incisor. The series is designated by H_3. Each section is represented by the encircled $\langle a_{gr} \rangle$-value and the double standard deviation added and subtracted. Ameloblastic and prismatic values are separated by a vertical line.

Fig. 12. Graphical representation of the ameloblastic and prismatic densities in a series of sections from a human tooth germ of a maxillary first deciduous incisor. The series is designated by H_4. Each section is represented by the encircled $\langle a_{gr} \rangle$-value and the double standard deviation added and subtracted. Ameloblastic and prismatic values are separated by a vertical line.

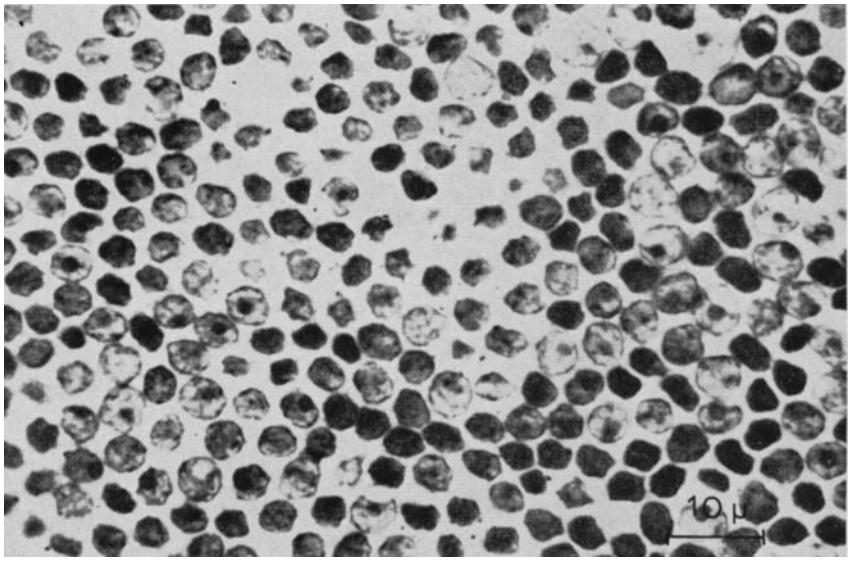

Fig. 13. Tangent section of the ameloblasts in a series from a feline tooth germ, photographed by 100× oil imm. obj.

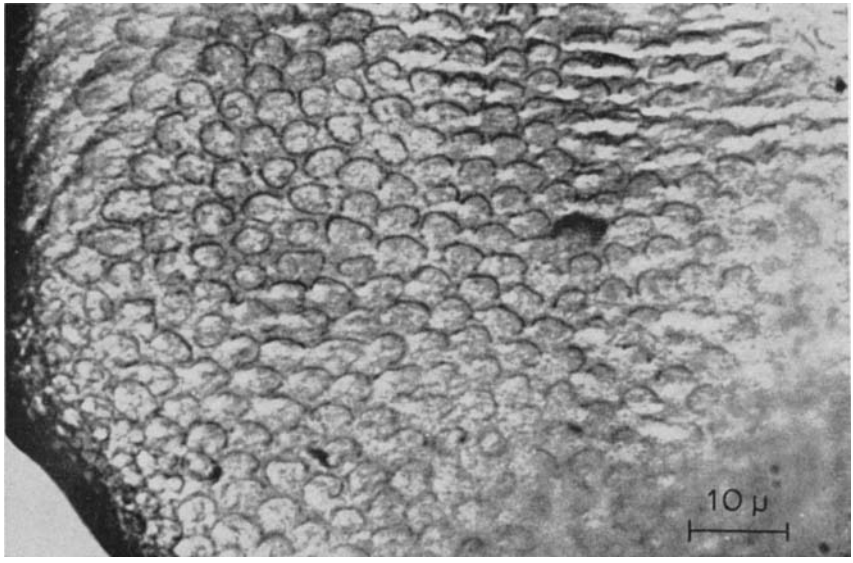

Fig. 14. Tangent section of the prisms in the same series whose ameloblasts were represented by Fig. 13. Photographed by 100× oil imm. obj.

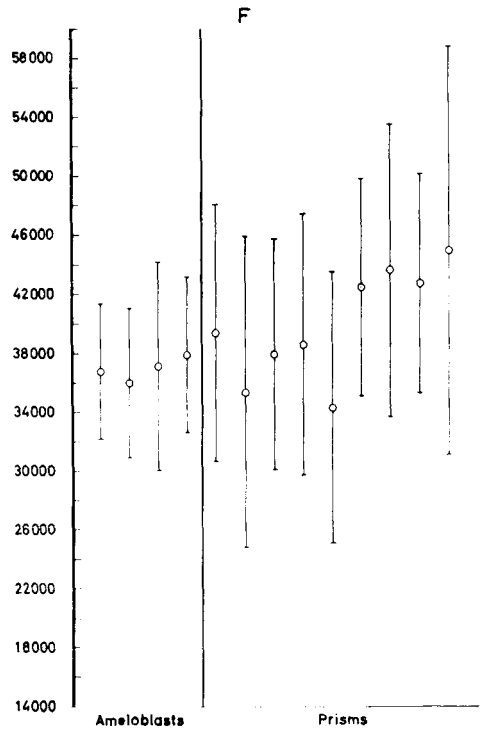

Fig. 15. Graphical representation of the ameloblastic and prismatic densities in a series of sections from a feline tooth germ of a deciduous incisor. The series is designated by F. Each section is represented by the encircled $\langle a_{gr} \rangle$-value and the double standard deviation added and subtracted. Ameloblastic and prismatic values are separated by a vertical line.

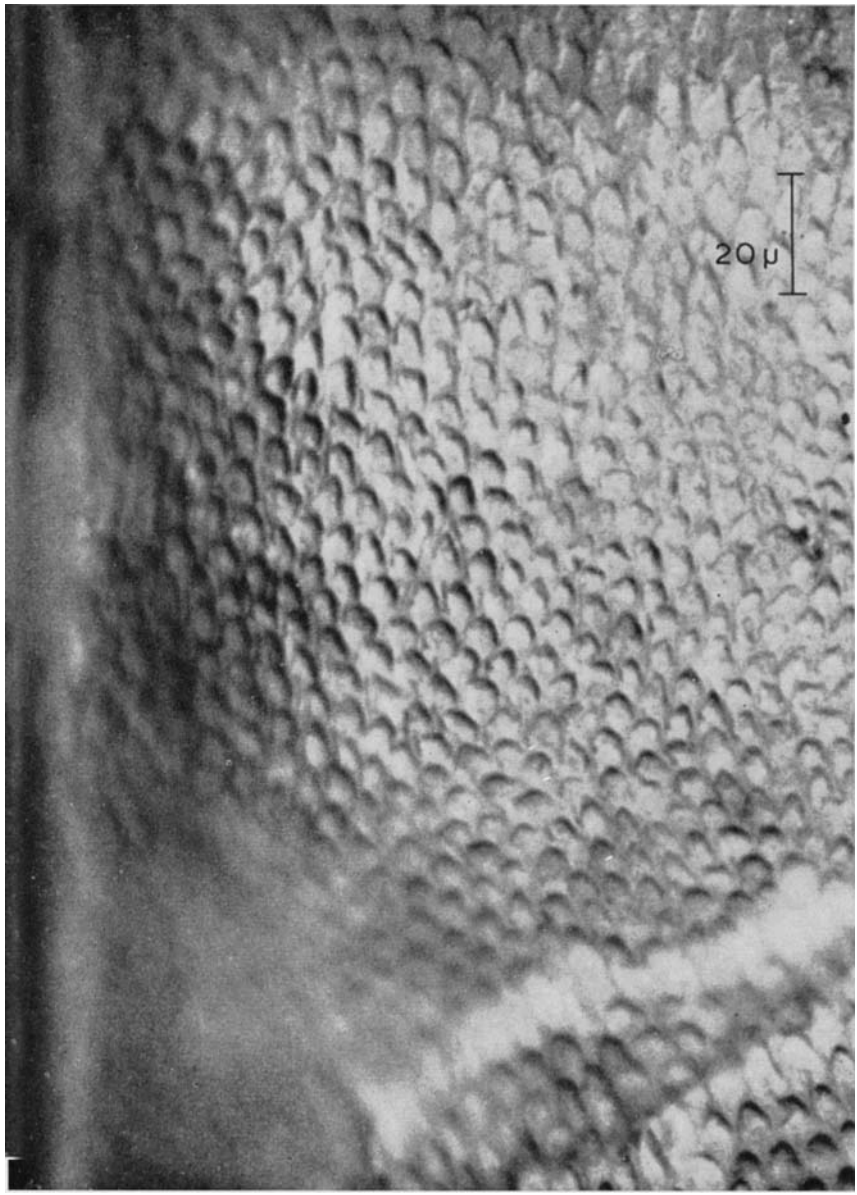

Figs. 16—19. The last four consecutive surfaces of a series of 20 etched surfaces in the labio-incisal enamel of a mature human maxillary first deciduous incisor. The interproximate distance between the etched surfaces was 5 μ in this series which is designated by i_1. The dentin was exposed in the last surface which is represented by Fig. 19.

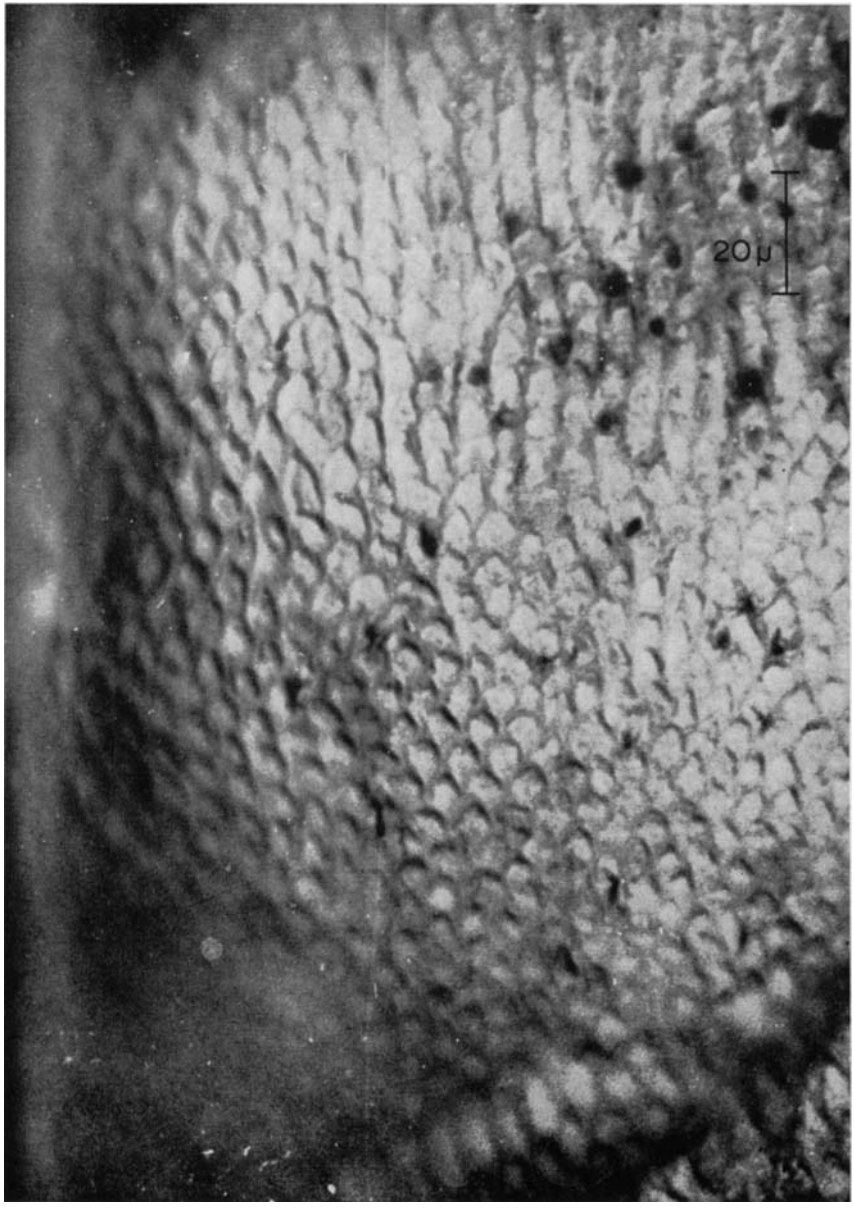

Fig. 17.

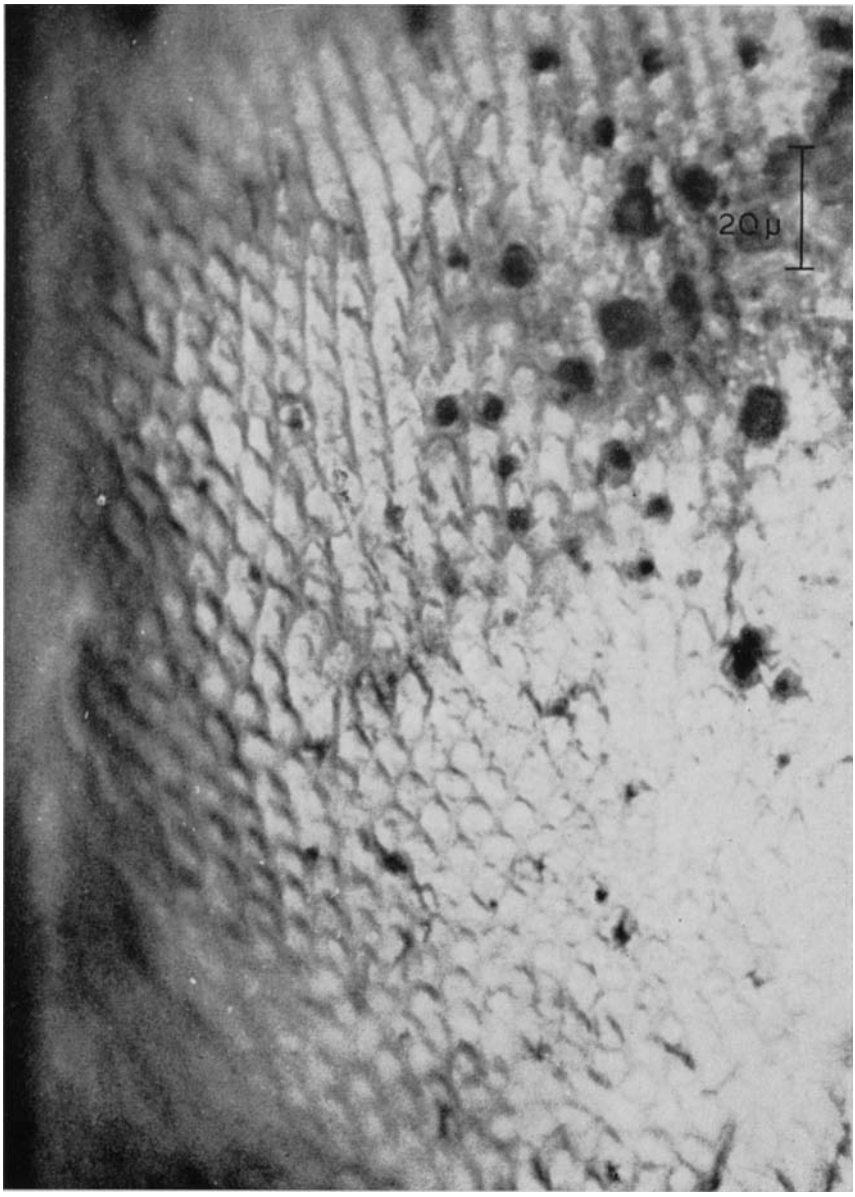

Fig. 18.

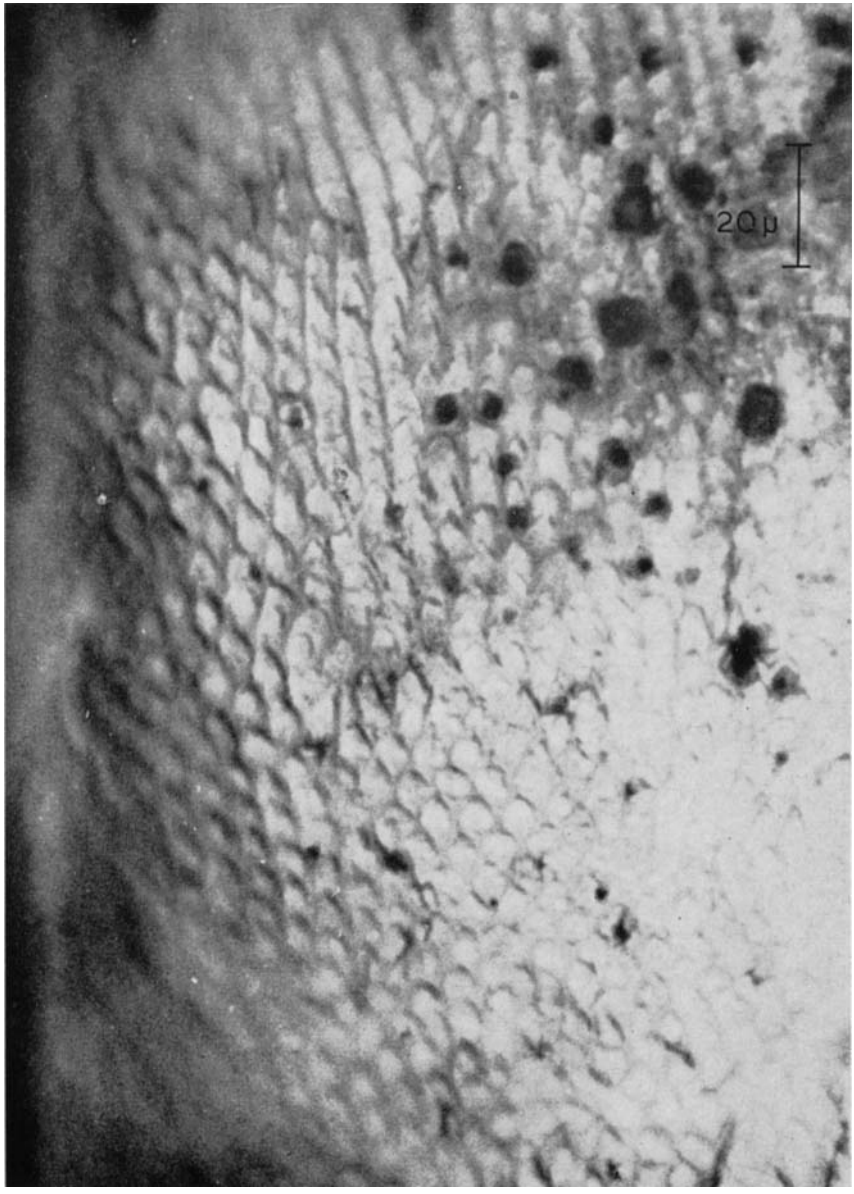

Fig. 19.

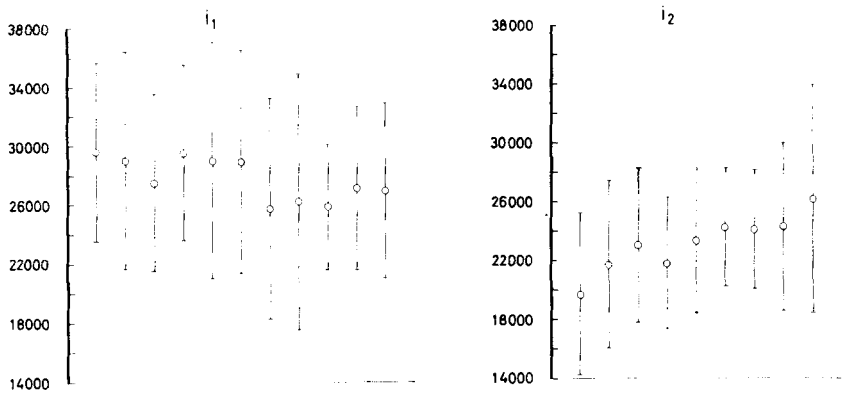

Fig. 20. Graphical representation of the prismatic density in a series of etched enamel surfaces from a mature human first deciduous incisor. The specimen is designated by i_1. Each surface is represented by the encircled $\langle a_{gr} \rangle$-value and the double standard deviation added and subtracted. The outer enamel surface is represented by the first $\langle a_{gr} \rangle$-value at the left-hand part of the graph.

Fig. 21. Graphical representation of the prismatic density in a series of etched enamel surfaces from a mature human first deciduous incisor. The specimen designated by i_2. Each surface is represented by the encircled $\langle a_{gr} \rangle$-value and the double standard deviation added and subtracted. The outer enamel surface is represented by the first $\langle a_{gr} \rangle$-value at the left-hand part of the graph.